

Informe Técnico Final

Proyecto CUDI "Red de estudio de sistemas nanométricos incluidos en materia suave para aplicaciones en Nanobiotecnología y Nanotecnología utilizando técnicas de corte en un Ultramicrotomo Criogénico de última generación".

En colaboración con la Dra. Patricia Santiago Jacinto, co-responsable del Proyecto se publicó el artículo (revista ISI):

- 1) Gold nanoparticles conjugated to Benzoylmercaptoacetyltryglycine and L-Cysteine methylester; *O. Estévez-Hernández, E.M. Molina-Trinidad, P. Santiago-Jacinto, L. Rendón, E. Reguera; Journal of Colloid and Interface Science 35 (2010) 161-167.* Se adjunta copia de este artículo;

Como resultados del mismo Proyecto, se encuentra en fase de arbitraje un segundo artículo, en particular:

- 2) Gold nanoparticles capped with Lanreotide peptide; *E.M. Molina-Trinidad, O. Estévez-Hernández, L. Rendón, V. Garibay-Febles, E. Reguera; Enviado a: Journal of Materials Science and Engineering C, se adjunta primera página del manuscrito.*
- 3) Se dispone de datos para escribir otros dos artículos que serán publicados en revistas internacionales ISI.

Otras Acciones Ejecutadas con apoyo del Proyecto.

- 1) Una estudiante de Doctorado (M. C. Blanca Zamora Reynoso) realizó un adiestramiento avanzado en la Universidad de Southampton, Inglaterra, con apoyo del Proyecto. A partir de los datos allí registrados se publicará un 3er artículo en revista ISI.
- 2) Un estudiante de Doctorado (M. C. Manuel Ávila Santos) ejecutó un proyecto de medición en el Laboratorio Nacional de Radiación Sincrotrón (LNLS) de Brasil, único de su tipo en el hemisferio sur. A partir de esos datos se publicara un 4to artículo ISI.
- 3) Con apoyo del Proyecto viajó al país en Profesor de la Universidad de Minnesota (Dr. Andreas Stein), el cual dictó una Conferencia Magistral en CICATA-IPN, Unidad Legaria, sobre la temática del Proyecto, y además participó en otras actividades académicas.

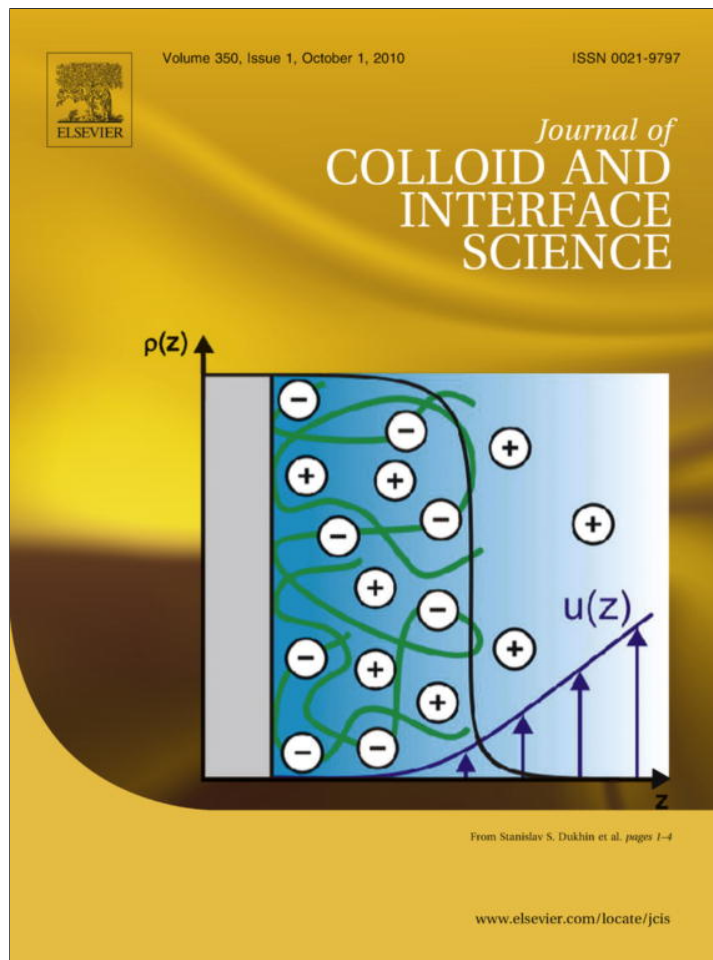
- 4) Con recursos del Proyecto se apoyó por 2 meses con 6 mil pesos /mes a la Dra. Adela Lemus Santana, recién egresada de la UNAM, y sin vínculo laboral o de posgrado, para que trabajara en la preparación de las muestras a estudiar, y como participante se le financió el boleto de avión para que asistiera a una Escuela de Verano sobre Nanotecnologías realizada en la Universidad de la Habana en Julio 2010.
- 5) Se apoyo a un estudiante de Doctorado (M. C. Jorge Roque de la Puente) para que asistiera a una Escuela Internacional sobre Nanotecnologías.
- 6) Se obtuvieron reactivos, material gastable e insumos generales para apoyar las tareas de investigación-desarrollo y formación de recursos humanos relativas al Proyecto.



Dr. Edilso Reguera

Responsable Técnico del Proyecto

Provided for non-commercial research and education use.
Not for reproduction, distribution or commercial use.



This article appeared in a journal published by Elsevier. The attached copy is furnished to the author for internal non-commercial research and education use, including for instruction at the authors institution and sharing with colleagues.

Other uses, including reproduction and distribution, or selling or licensing copies, or posting to personal, institutional or third party websites are prohibited.

In most cases authors are permitted to post their version of the article (e.g. in Word or Tex form) to their personal website or institutional repository. Authors requiring further information regarding Elsevier's archiving and manuscript policies are encouraged to visit:

<http://www.elsevier.com/copyright>



Contents lists available at ScienceDirect

Journal of Colloid and Interface Science

www.elsevier.com/locate/jcis



Gold nanoparticles conjugated to benzoylmercaptoacetyltriglycine and L-cysteine methylester

O. Estévez-Hernández^{a,b}, E.M. Molina-Trinidad^{a,c}, P. Santiago-Jacinto^d, L. Rendón^d, E. Reguera^{a,b,*}^a Centro de Investigación en Ciencia Aplicada y Tecnología de Avanzada, IPN, Legaria 694, México DF, Mexico^b Instituto de Ciencia y Tecnología de Materiales, Universidad de La Habana, Cuba^c Facultad de Estudios Superiores Cuautitlán, Universidad Nacional Autónoma de México, Estado de México, Mexico^d Instituto de Física, Universidad Nacional Autónoma de México, México DF, Mexico

ARTICLE INFO

Article history:

Received 22 April 2010

Accepted 19 June 2010

Available online 25 June 2010

Keywords:

Gold nanoparticles

Benzoylmercaptoacetyltriglycine

L-cysteine methylester

Capping agents

ABSTRACT

Benzoyl-protected mercaptoacetyltriglycine, a synthetic precursor used in the preparation of Technetium-99 m-mercaptoacetyltriglycine, a radiopharmaceutical for renal tubular function and L-cysteine methylester, a small, non-zwitterionic amino acid derivative, were used as capping agents of gold nanoparticles obtained by borohydride reduction method. The capped gold nanoparticles composites were prepared from aqueous solutions and characterized by UV–Vis, infrared and Raman spectra and Transmission Electron Microscopy images. The presence of the ligands and its different binding mode to the particles as a consequence of the benzoyl-protection of the thiol group in benzoyl-protected mercaptoacetyltriglycine were evidenced from infrared and Raman spectra. The stability on aging in water solution of the formed composites is discussed from the obtained UV–Vis spectra.

© 2010 Elsevier Inc. All rights reserved.

1. Introduction

The applications of surface functionalized metal nanoparticles have been explored in a wide variety of areas [1]. Colloidal gold nanoparticles (AuNPs) have found technologically uses since ancient times related to their optical properties, but only in the last decades their potential biological applications in labeling, delivering, heating and sensing processes have been demonstrated [2–5]. Among noble metal particles, AuNPs have attracted intensive attention related to their easy preparative routes available, their low toxicity, and the gold surface affinity for the bonding to molecules of biological interest [5,6]. Gold and other noble metal nanoparticles have great potential for applications in biochemical sensing and biological imaging because of their unique optical properties originated from the excitation of local surface plasmon resonances [7,8]. The surface plasmon resonance is a coherent oscillation of the surface conduction electrons excited by electromagnetic radiation. It is sensitive to the local dielectric environment [9]. Typically, local surface plasmon resonances devices sense changes in the local environment through a shift for the resonance wavelength. Apart from the environmental effect, the surface resonance plasmon of nanoparticles is dramatically affected by their size, shape, and surface modifications [7,10]. The highly confined local electric field enhancement

that accompanies the excitation of the plasmon supports variety spectroscopic and imaging techniques [11–13].

The synthesis of AuNPs with diameters ranging from a few to several hundreds of nanometers in aqueous solution as well as in organic solvents is well established [10,14–17]. In typical syntheses, Au salts are reduced by addition of a reducing agent such as sodium citrate or borohydride. In addition, a stabilizing agent (surfactant) is also required which is either adsorbed or chemically bound to the surface of AuNPs. The surfactant is typically charged, so that the equally charged NPs repel each other so that they remain stable in colloidal state. Most biological or biomedical applications require that the clusters readily dissolve in aqueous media which is favored if the aggregation is prevented through electrostatic interactions. Biological molecules can be attached to the particles in several ways. If the biological molecules have a functional group which can bind to the Au surface (like thiols, cyano, amino or specific peptide sequences), the biological molecules can replace some of the original stabilizer molecules when they are added directly to the particles solution. Studies on the interaction of Au with biomolecules is an active research area where useful information is being obtained [18,19]. Benzoyl-protected mercaptoacetyltriglycine (BzMAG₃) is a synthetic ligand used in the preparation of Technetium-99 m-mercaptoacetyltriglycine, a radiopharmaceutical for renal tubular function [20]. From the conjugation of AuNPs to BzMAG₃ a useful tool for imaging or diagnostic of renal tubular function could be obtained. Furthermore, it opens up several novel possibilities as the BzMAG₃ structure could be derivatized because of its free carboxylic group. Different active groups capable of performing specific functions like

* Corresponding author at: Centro de Investigación en Ciencia Aplicada y Tecnología de Avanzada, IPN, Legaria 694, México DF, Mexico. Fax: +52 55 53954147.

E-mail address: ereguera@yahoo.com (E. Reguera).

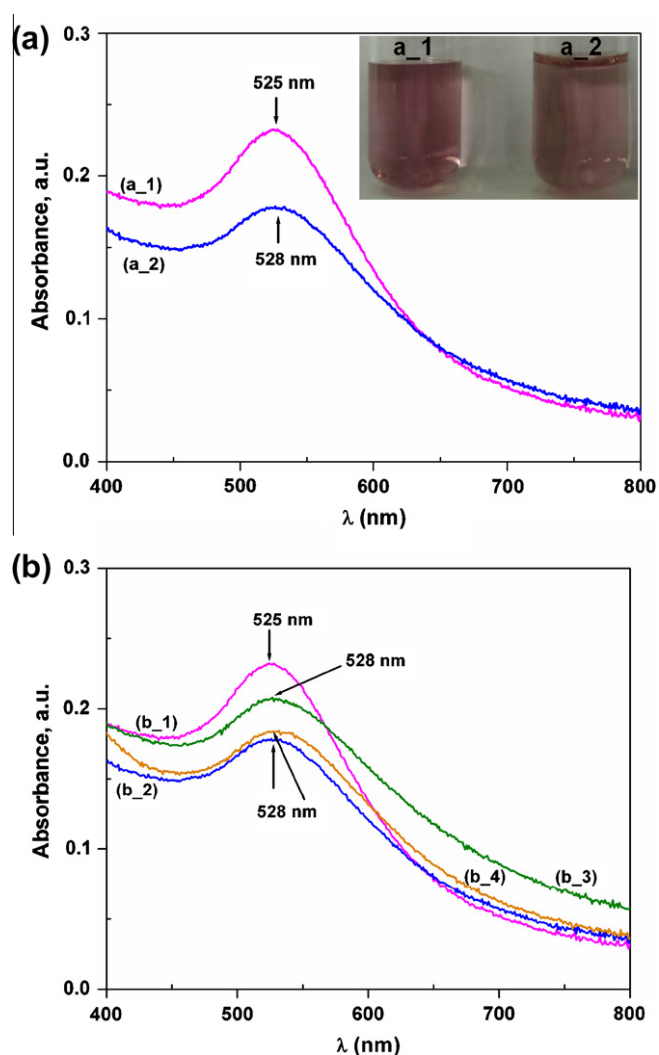


Fig. 2. UV-Vis spectra for: (a) AuNPs (a₁) and Au@BzMAG₃ (a₂); (b) AuNPs (b₁) and Au@BzMAG₃ (b₂) solutions as freshly prepared and after 30 days of aging (b₃ and b₄, respectively).

two potential anchoring groups (SH and NH₂) that can covalently bind Au particles, it is well established the superiority of thiol group to form covalent bond with gold [28]. Because in CysM the thiol terminal group is free, this simple cysteine derivative may be useful to sense comparatively the interaction with Au surface relative to the less accessible benzylmercapto group in BzMAG₃. As already-mentioned, in the CysM the existence of zwitterion (internal salt) is not possible because the carboxylic group is derivatized as methylester. This fact hinders the nanoparticles assembling through the zwitterions-type electrostatic interactions, which is observed for instance when cysteine is used as capping ligand [22].

Freshly prepared AuNPs obtained by sodium borohydride reduction are stable in water and display a characteristic UV-Vis absorption spectrum with a plasmon band in the 522–525 nm spectral range (curves a₁ of Figs. 2a and 3a). On aging, a noticeable red shift accompanied of the peak broadening is observed (discussed below). As already-mentioned, the plasmon resonance absorption is sensitive to the particles environment. Such effect was used to sense the AuNPs conjugation to the two considered capping ligands. For BzMAG₃ a slight red shift, from 525 to

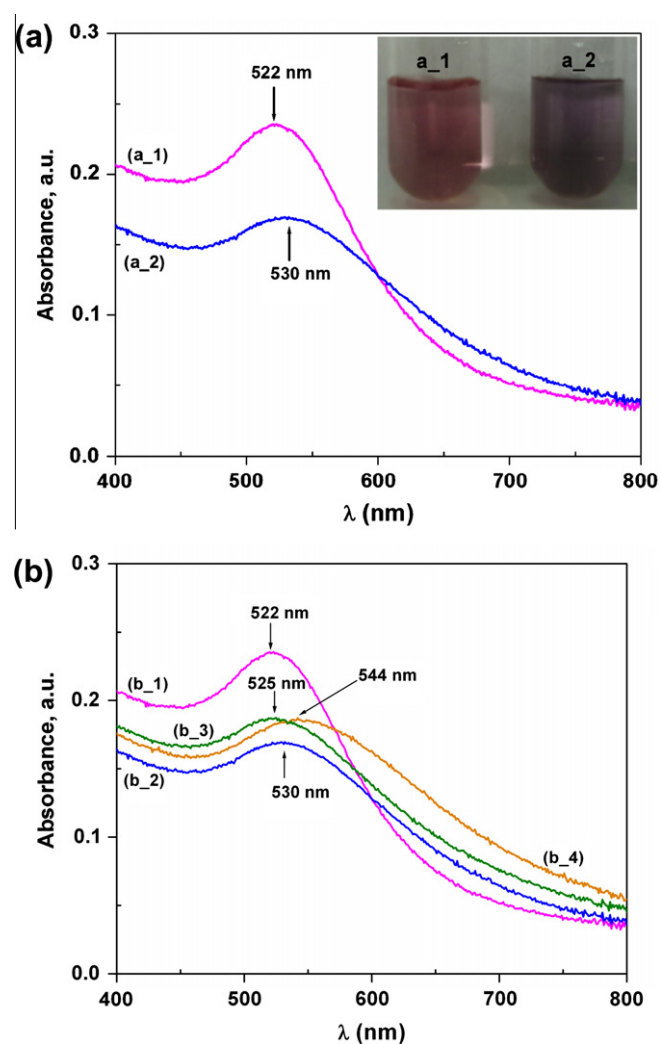


Fig. 3. UV-Vis spectra for: (a) AuNPs (a₁) and Au@CysM (a₂); (b) AuNPs (b₁) and Au@CysM (b₂) as freshly prepared solutions, and after 30 days of aging (b₃ and b₄, respectively).

528 nm, together of certain peak broadening and a decrease of its maximum absorbance were detected (curve a₂ in Fig. 2a). Such spectral variations, without appreciable color changes, were interpreted as resulting from the BzMAG₃ binding to the Au surface. A quite different behavior was observed for the CysM ligand interaction with AuNPs. In this case the red shift for the plasmon resonance peak was significantly greater, of about 8 nm (from 522 nm to 530 nm) and the peak broadening is accompanied of a color change for the colloidal suspension, from ruby-red to blue (curve a₂ in Fig. 3a).

Such color change in colloidal gold has been ascribed to formation of AuNPs aggregates [29]. The observed differences in behavior for the interactions of these two ligands with AuNPs were interpreted as related to the nature of the electrostatic interaction involved between the capped gold particles; CysM is uncharged and this ligand de-stabilizes the suspension by reducing the electrostatic repulsion between the gold particles when it adsorbs. In contrast BzMAG₃ is negatively charged (carboxylic group) in solution at most pH values above four (the measured pH of the mixture reaction is about 8–9), and when adsorbed through the amine groups, will retain this negative charge upon adsorption, thus maintaining the electrostatic repulsion between AuNPs. The stability of BzMAG₃ and CysM capped AuNPs in comparison with

¹ For interpretation of color in Figs. 2 and 3, the reader is referred to the web version of this article.

free Au colloid for a month of aging was also studied. For Au@Bz-MAG₃ composite, the wavelength where the plasmon peak maximum is observed remains stable at 528 nm (curves b_2 and b_4 of Fig. 2b) and without significant peak broadening. This was interpreted as formation of a stable composite where the capped nanoparticles preserve their colloidal state (no aggregates formation). Such behavior results appropriate for potential applications of that composite for imaging and diagnostic tool. Relative to Au@Bz-MAG₃ the formed Au@CysM composite shows quite different features on aging, and also different to those observed for non-conjugated Au colloidal suspension. On the Au@CysM aging a gradual red shift from 530 to 544 nm accompanied of peak broadening was observed for the plasmon resonance signal (curves b_2 and b_4 of Fig. 3b). This was attributed to a progressive nanoparticles aggregation process. It seems the capped nanoparticles interact through attractive dispersive forces maintaining several nanoparticles together. Such mechanism must be quite different to that reported for the aggregation of AuNPs capped with cysteine ligand [22]. As already-mentioned, with cysteine the aggregation process takes place through zwitterion-type electrostatic interactions, mechanism that is not possible for CysM.

The above discussed UV–Vis results were supported by qualitative information on the chemical composition of the formed composite nanoparticles. From the colloidal suspension nanoparticles were separated from the mother solution by centrifugation, and then washed several times with distilled water. For the obtained powder of dried nanoparticles EDS spectra were recorded. Without exception, in all the spectra X-ray peaks corresponding to S and Au were observed (see Supplementary information), although this fact is not a definitive proof that the capping agent is adsorbed and intact. Many thiol systems are known to undergo oxidation and C–S bond scission once adsorbed [30].

Conventional and High Resolution TEM (HRTEM) images were used to obtain structural information on Au@Bz-MAG₃ and Au@CysM composites. For Au@Bz-MAG₃ HRTEM images revealed nanoparticle sizes with mean diameters in the 2–7 nm range (Fig. 4a and b). The HRTEM images also show that these nanoparticles are single crystalline, as clearly indicated by atomic lattice fringes (Fig. 4b) and the corresponding interatomic planes distance which match to the {1 1 1} family of planes.

On the other hand, a difference in contrast observed around isolated nanoparticles of Au@CysM composite suggests the presence of CysM linked to the Au surface (Fig. 5a).

For non-aged Au@CysM colloidal solutions (Fig. 5b), the mean particle diameter was found to be in the 2–9 nm range for non-aged

Au@CysM colloidal solutions (Fig. 5b). HRTEM micrographs show that small nanoparticles are single crystalline, but the bigger ones have structural defects (Fig. 5c) as is indicated by the FFT of the particle. The most common family of planes observed corresponds to {1 1 1}. Nevertheless, even for samples without significant aging, the HRTEM images revealed a marked trend to aggregates formation (Fig. 5c), which is more pronounced when the sample is exposed for some minutes to the electron beam effect.

The vibrational spectrum of molecular species is affected by its interaction with a given surface. From this fact the IR and Raman spectra can be used as sensors for Bz-MAG₃ and CysM bonding to the gold particles surface. In addition, the vibrational spectrum contains information on the functional groups available in the considered molecule and this allows their identification and possible interactions through the corresponding absorption band positions (vibration frequencies). From the IR spectrum valuable information on nature of the bonding interactions that are involved in the Au@Bz-MAG₃ and Au@CysM composites formation was obtained. Usually IR and Raman spectra of the ligands-capping nanoparticles are compared to those obtained from the free ligands.

The frequency shift and changes in the bands intensity corresponding to the ligand functional groups serve as sensor of those groups that are participating in the bonding interactions. Fig. 6 shows the IR spectra for Au@Bz-MAG₃ and Bz-MAG₃ as free ligand, respectively. In general, both spectra are similar, although the ligand shell formation contributes to the broadening and blurring of spectral features. These are typical changes reported in the literature for ligands–surface interactions [31–36]. For Bz-MAG₃ such changes were interpreted as evidence of occurrence of a bonding interaction to the surface of AuNPs. For Bz-MAG₃ backbone the infrared-active modes are expressed in the amide bands [31]. The frequency changes for these bands are evident when the two spectra are compared (Table 1, Fig. 6). The N–H stretching bands fall in 3300 cm⁻¹, for free NH, and at 3083 cm⁻¹, for associated NH. In compounds containing the amide groups (HNCO) these fundamentals are known as Amide bands A and A' [31,32,36,37], respectively. Nevertheless, for Bz-MAG₃ the Amide A' band could be merged with the aromatic CH stretch band of the benzoyl group. It can be inferred from the recorded spectra (Fig. 6) that the secondary amide functions participate in the bonding of the ligand to the surface, as already found by other authors for peptides [31,36,37]. This is concluded from the shift of the centered secondary amide band from 3300 cm⁻¹ in the free Bz-MAG₃ ligand (spectrum a) to 3437 cm⁻¹ in the Au@Bz-MAG₃ composite (spectrum b). Besides the A' band at 3083 cm⁻¹ is absent in the spectrum of the Au@Bz-MAG₃. The

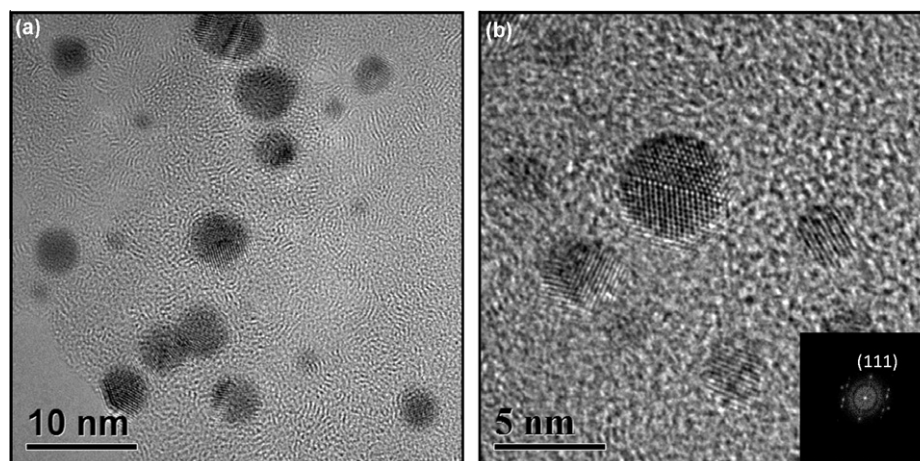


Fig. 4. HRTEM images of Au@Bz-MAG₃ composite: (a) conventional TEM micrograph showing the 2–7 nm size range of the particles; (b) image of Au@Bz-MAG₃ and the corresponding FFT that shows {1 1 1} reflection of crystal planes for Au.

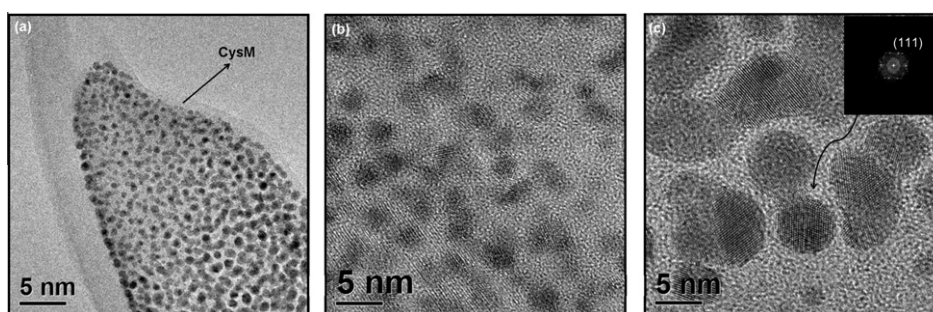


Fig. 5. (a) Conventional TEM micrograph showing the AuNPs embedded in the CysM layer; (b) HRTEM image of isolated Au@CysM nanoparticles of size in the 2–9 nm range; (c) Au@CysM and the corresponding FFT that shows {1 1 1} reflection of crystal planes for Au.

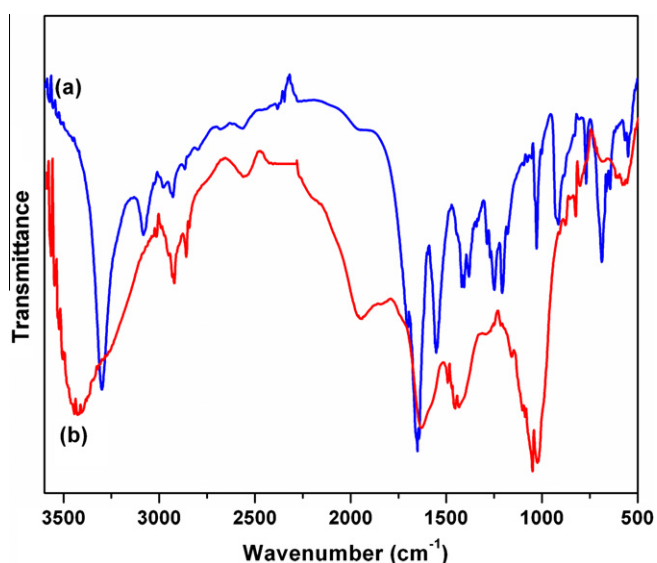


Fig. 6. IR spectra for BzMAG₃ (spectrum a) and Au@BzMAG₃ (spectrum b).

broadening observed in this spectral region (3500–2500 cm⁻¹) was attributed to the contribution from the O–H stretching vibrations of carboxylic groups. The band observed in the free ligand as a shoulder at 1703 cm⁻¹ (spectrum a) corresponds to C=O stretching vibration from carboxylic groups [20,38]. For the Au@BzMAG₃ (spectrum b) that band is not observed because of the mentioned spectral broadening on the surface complex formation. On the other hand, the Amide I band have a large contribution of from C=O stretching motion [36,38] and it appears as a broad intense band which shifts from 1645 to 1636 cm⁻¹ on the conjugate formation. This was interpreted as evidence that carbonyl groups are not

participating in the BzMAG₃ bonding to the gold particles surface. The Amide II band that have contributions of both N–H in-plane bending and C–N stretching [36,38] centered near 1552 cm⁻¹ is not observed in the Au@BzMAG₃ IR spectrum. This suggests a probable interaction of the secondary amide groups with the gold surface [36].

Infrared-active modes attributed to skeletal motions and out-of-plane vibrations from the substituent groups include C–H stretching modes of the CH₂ groups at 2939 (asymmetric), 2867 (symmetric) cm⁻¹ and OH deformation of the carboxylic group at 1419 cm⁻¹ [20,38]. An aromatic C–C stretching at 1208 and C–H out of plane deformation at 664 cm⁻¹ were assigned to the aromatic benzene ring of the benzoyl group [20,38]. Although these infrared modes are conserved in the Au@BzMAG₃ composite formation (spectrum a), the majority of the bands in the 1500–500 cm⁻¹ region are broad, blurred and reduced in intensity. This indicates that the interaction of the BzMAG₃ ligand with gold surface produces a global change in the ligand electronic structure. The C–S stretching vibration in the free ligand (BzMAG₃, spectrum a) was localized at 612 cm⁻¹ [38] but not observed once the Au@BzMAG₃ composite is formed (spectrum b).

Fig. 7 shows the IR spectra of CysM and Au@CysM. The bands observed in the spectra (Table 1) were identified as follow: the weak band for CysM (spectrum a) at 3469 cm⁻¹ corresponds to N–H stretching mode of the amino group [38,39]. The bands in the 3250–2750 cm⁻¹ region are broad, but it was possible to be assigned to C–H asymmetric stretching of the methyl group at 2954 cm⁻¹ and the C–H symmetric stretching of the methylene group at 2857 cm⁻¹ [38–40]. Fortunately, the S–H stretching vibration was visible in the IR spectrum of free CysM (spectrum a, black arrow) as a very weak band near 2561 cm⁻¹ [21,38,40]. The most intense band at 1741 cm⁻¹ was assigned to the C=O stretching [38–40]. A band at 1515 cm⁻¹ was ascribed to N–H bend [38]. Another infrared-active modes include the C–O, C–N

Table 1

Infrared spectral mode assignments of BzMAG₃, Au@BzMAG₃, CysM and Au@CysM.

| BzMAG ₃ | Au@BzMAG ₃ | Assignment | CysM | Au@CysM | Assignment |
|--------------------|-----------------------|---------------------------------|------|---------|---------------------------------|
| 3300 ^a | 3437 | Amide A | 3469 | 3451 | NH str |
| 3083 | | Amide A | 2954 | | CH ₃ V _{as} |
| 2939 | 2929 | CH ₂ V _{as} | | 2928 | CH ₂ V _{as} |
| 2867 | 2866 | CH ₂ V _s | | 2865 | CH ₃ V _s |
| 1703 | | C=O str | 2857 | | CH ₂ V _s |
| 1645 | 1636 | Amide I | 2561 | | SH str |
| 1552 | 1497 | Amide II | 1741 | 1733 | C=O str |
| 1419 | 1439 | OH def | 1515 | 1497 | NH def |
| 1208 | | C–C str (aromatic) | 1246 | | CO str |
| 1028 | 1054 | CO str | 1075 | 1054 | CN str |
| 664 | | CH def | 616 | 619 | CS str |

^a Values in cm⁻¹.

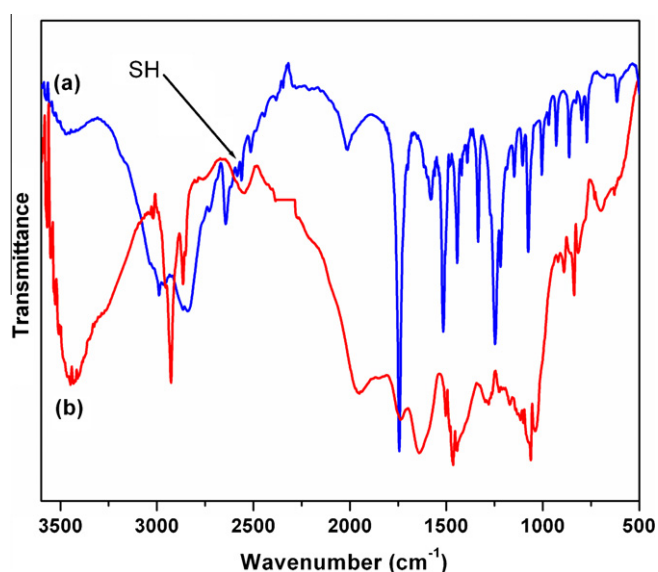


Fig. 7. IR spectra for CysM (spectrum a) and Au@CysM (spectrum b).

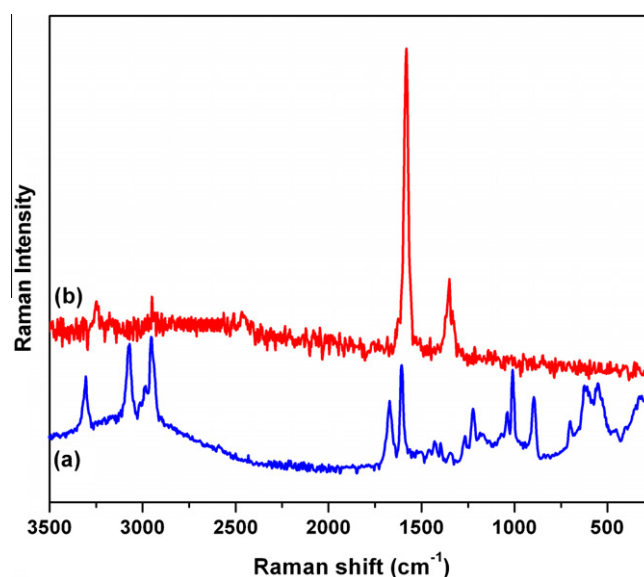


Fig. 8. Raman spectra for BzMAG₃ (spectrum a) and Au@BzMAG₃ (spectrum b).

and C—S stretching at 1246, 1075 and 616 cm^{-1} , respectively [38]. The Au@CysM composite formation leads to some spectral changes relative to the free ligand (CysM), such as broadening, reduction and increase for the intensity of various bands (spectrum b). The band of the N—H stretching appears broader and it was slightly shifted to lower frequency (3451 cm^{-1}). It indicates that the amino group is not involved in the interaction with the AuNPs surface. However, the bands corresponding to stretches of C—H groups (methyl and methylene) were sharper. These two bands were assigned as asymmetric stretching of the methylene group at 2928 cm^{-1} symmetric stretching of the methyl group at 2865 cm^{-1} . It seems the interaction of the CysM with gold surface changes the active modes of vibration of methyl and methylene groups, probably due to the nearby of the methylene fragment to the SH group. Similar changes were observed in the IR spectrum of the cysteine capped gold nanoparticles where the bands of the CH₂ group of cysteine ligand is absent [21]. The weak band of the S—H stretching mode at 2561 cm^{-1} is not seen for the Au@CysM and this confirms the S—Au bond formation. On the other hand, the band of the C=O stretching appears as a broad band that slightly shifts to lower energy (1733 cm^{-1}). All these spectral changes support the CysM bonding to the Au surface through the terminal thiol group [21].

Raman spectra were also recorded in order to compare the different vibration modes for free BzMAG₃ and CysM ligands and in the Au@BzMAG₃ and Au@CysM composites. Signals from motions of heavy atoms (with a highly polarizable electronic structure) appear with relatively high intensity in the Raman spectra. In consequence, vibrations involving motions of the C—S and S—H groups will be present in Raman spectra with a more prominent intensity than in IR spectra. These facts have been used specially to investigate the mercapto bonds in the conjugated samples. Concerning to the number of bands and their intensity, the Raman spectra are simpler. In Fig. 8 the Raman spectra of the BzMAG₃ (spectrum a) and Au@BzMAG₃ (spectrum b) are shown. It is clear from these spectra that after conjugation with AuNPs several bands of BzMAG₃ disappear (spectrum b). The doublet representing the Amide A and A' bands from N—H stretching mode was localized at 3298 and 3066, respectively in free BzMAG₃ (spectrum a). The N—H stretching vibration for Au@BzMAG₃ (spectrum b) was found at 3248 cm^{-1} . This weak band is probably a combination of the Amide bands A and A' after the interaction with the gold surface.

The band at 2947 cm^{-1} in the BzMAG₃ (spectrum a) was assigned to the symmetric stretching of the CH₂ groups. This vibration appears in the conjugate as a weak band at 2951 cm^{-1} . Other significant bands in the BzMAG₃ spectrum are the Amide band I (C=O stretching mostly) at 1666 cm^{-1} , an aromatic C—C stretching from the benzoyl group at 1601 and 1218 cm^{-1} , a trigonal ring “breathing” from the monosubstituted benzene at 1005 cm^{-1} , the C—N stretching at 891 cm^{-1} and the C—S stretching at 603 cm^{-1} , respectively [38].

The two most intense Raman bands for Au@BzMAG₃ (Fig. 8, spectrum b) were observed at 1581 and 1350 cm^{-1} assigned to aromatic C—C stretching from the benzoyl group and Amide III band, a more-complex combination of C=O and C—N stretchings, respectively. The Amide I band (C=O stretching mostly) observed in the free ligand at 1666 cm^{-1} is absent for the conjugated; however, the Amide III band appears with a relatively high intensity for Au@BzMAG₃. Such spectral change on the surface complex formation was interpreted as resulting from a symmetry change for BzMAG₃ caused by its interaction with the surface of AuNPs. This agrees with the above discussed results from IR spectra.

Raman spectra were also recorded for CysM and Au@CysM (Fig. 9). The spectrum (a) of CysM shows the C—H asymmetric and asymmetric stretching modes of the methyl and methylene groups at 2955 and 2868 cm^{-1} , respectively. The band attributed to thiol group S—H was observed at 2561 cm^{-1} [21]. Additionally, C=O stretching mode of the methylester fragment and the C—N band were detected at 1741 and 859 cm^{-1} , respectively. Two bands from the C—S stretching mode were detected at 675 cm^{-1} and 612 cm^{-1} [38]. The Raman spectrum of the Au@CysM-A (b in Fig. 9) shows only two intense bands at 2885 and 2850 cm^{-1} attributed to symmetric C—H stretching of the methyl and methylene groups, respectively [21,38].

Additionally, a weak band at 1457 cm^{-1} due to the usual superposition of the scissor deformation motion of the methylene group and the asymmetric bending of the methyl group was observed [38]. The S—H stretch is absent for the conjugated product confirming the S—Au coordination bond formation, a spectral feature already-reported for other molecules containing the S—H when they are coordinated to gold surface [21,25]. Significantly, the C=O stretching is no longer seen in the spectrum of Au@CysM, nevertheless, the O—Au interaction is discarded from IR spectra. The base line of the spectrum exhibits a pronounced enhancement

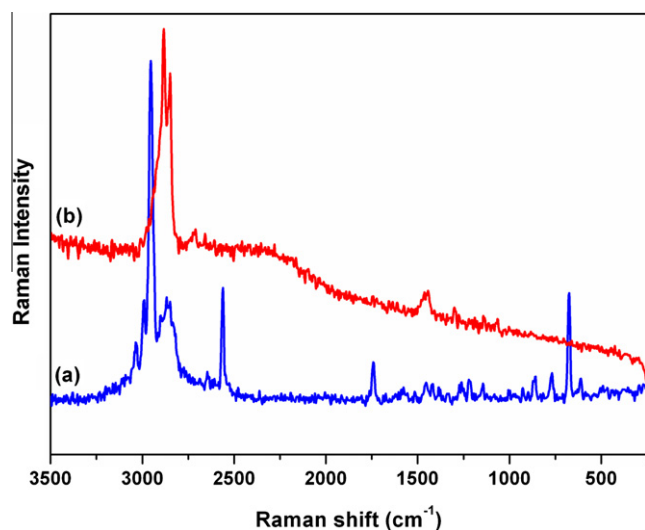


Fig. 9. Raman spectra for CysM (spectrum a) and Au@CysM (spectrum b).

of the Raman intensity. It is known that molecules adsorbed at roughened noble metal surfaces can show the surface-enhancement Raman scattering (SERS) effect [11]. This fact is another evidence of the effective CysM conjugation to AuNPs.

4. Conclusions

In this contribution, a systematic study to identify the possible conjugation of AuNPs to BzMAG₃ and CysM capping ligands was carried out. UV–Vis spectra were used as primary sensor for the Au@Bz-MAG₃ and Au@CysM composites formation. For BzMAG₃ the obtained conjugate results stable in aqueous solution for at least a month of aging, a behavior quite different to that observed for Au@CysM where evidence of aggregation was obtained. The change in color on aging for the formed Au@CysM composite also suggests the appearance of nanoparticles aggregates. These results from UV–Vis were also suggested by the structural study from TEM and HRTEM images. IR and Raman spectra provided conclusive information on those functional groups involved in the bonding with the gold particles surface. For BzMAG₃ the amide groups are able to interact with gold because the mercapto group is benzoyl-protected. However, for CysM the free thiol moiety is available to form a coordination bond and, in consequence, it results a very effective site to interact with gold. The results herein discussed are considered as preliminary for a more advanced study on the potential applications of Au@BzMAG₃ composite as an imaging and diagnostic tool for renal tubular function.

Acknowledgments

This research was supported by the National Council of Science and Technology (CONACYT-MÉXICO, Research grant 61541). The authors are thankful to Dr. Vicente Garibay-Febles and Instituto

Mexicano del Petróleo for providing us the electron microscopy facilities used in this study.

Appendix A. Supplementary material

Supplementary data associated with this article can be found, in the online version, at doi:10.1016/j.jcis.2010.06.051.

References

- [1] S. Bhat, U. Maitra, *Chem. Mater.* 18 (2006) 4224.
- [2] P. Sharma, S. Brown, G. Walter, S. Santra, B. Moudgil, *Adv. Colloid Interface Sci.* 123–126 (2006) 471.
- [3] G.F. Paciotti, D. Weinreich, D. Goia, N. Pavel, R.E. McLaughlin, L. Tamarkin, *Drug Delivery* 11 (2004) 169.
- [4] R. Wilson, *Chem. Soc. Rev.* 37 (2008) 2028.
- [5] R. Sperling, P. Rivera Gil, F. Zhang, M. Zanella, W.J. Parak, *Chem. Soc. Rev.* 37 (2008) 1896.
- [6] E.E. Connor, J. Mwamuka, A. Gole, C.J. Murphy, M.D. Wyatt, *Small* 1 (2005) 325.
- [7] K.A. Willets, R.P. Van Duyne, *Annu. Rev. Phys. Chem.* 58 (2007) 267.
- [8] Y. Chen, J.A. Preece, R.E. Palmer, *Ann. N.Y. Acad. Sci.* 1130 (2008) 201.
- [9] M.M. Miller, A.A. Lazarides, *J. Phys. Chem. B* 109 (2005) 21556.
- [10] J. Kimling, M. Maier, B. Okenve, V. Kotaidis, H. Ballot, A. Plech, *J. Phys. Chem. B* 110 (2006) 15700.
- [11] C.D. Keating, K.M. Kovaleski, M.J. Natan, *J. Phys. Chem. B* 102 (1998) 9404.
- [12] J. Zhang, Y. Fu, J.R. Lakowicz, *J. Phys. Chem. C* 111 (2007) 50.
- [13] T. Li, L. Guo, Z. Wang, *Anal. Sci.* 24 (2008) 907.
- [14] T. Jennings, G. Strouse, *Bio-applications of Nanoparticles*, vol. 620, Springer Science+Business Media, New York, 2007, p. 34.
- [15] J. Turkevich, P.C. Stevenson, J. Hillier, *Discuss. Faraday Soc.* 11 (1951) 55.
- [16] M. Brust, M. Walker, D. Bethell, D.J. Schiffrin, R. Whyman, *J. Chem. Soc., Chem. Commun.* 34 (1994) 801.
- [17] N.R. Jana, X. Peng, *J. Am. Chem. Soc.* 125 (2003) 14280.
- [18] J.R. Siqueira Jr., L. Caseli, F.N. Crespilho, V. Zucolotto, O.N. Oliveira Jr., *Biosens. Bioelectron.* 25 (2010) 1254.
- [19] L. Wang, S. Song, D. Pau, D. Li, C. Fan, *Pure Appl. Chem.* 82 (2010) 81.
- [20] A.R. Frtzbeg, S. Kasina, D. Eshima, L.D. Johnson, *J. Nucl. Med.* 27 (1986) 111.
- [21] S. Aryal, B.K.C. Remant, N. Dharmaraj, N. Bhattarai, C.H. Kim, H.Y. Kim, *Spectrochim. Acta, Part A* 63 (2006) 160.
- [22] A. Mocanu, I. Cernica, G. Tomoaia, L.-D. Bobos, O. Horovitz, M. Tomoaia-Cotisel, *Colloids Surf., A* 338 (2009) 93.
- [23] I. Ojéa-Jiménez, V. Puentes, *J. Am. Chem. Soc.* 131 (2009) 13320.
- [24] A. Majzik, R. Patakfalvi, V. Hornok, I. Dékány, *Gold Bull.* 42 (2009) 113.
- [25] I. Patean, G. Tomoaia, O. Horovitz, A. Mocanu, M. Tomoaia-Cotisel, *J. Optoelectron. Adv. Mater.* 10 (2008) 2289.
- [26] L. Reyes-Herrera, G. Ferro-Flores, J. Lezama-Carrasco, M.A. Gonzalez-Zavala, F. Ureña-Núñez, E. Avila Ramirez, *J. Radioanal. Nucl. Chem., Lett.* 199 (1995) 507.
- [27] V. Patil, R.B. Malvankar, M. Sastry, *Langmuir* 15 (1999) 8197.
- [28] P.V. Bower, E.A. Louie, J.R. Long, P.S. Stayton, G.P. Drobny, *Langmuir* 21 (2005) 3002.
- [29] K.S. Mayya, V. Patil, M. Sastry, *Langmuir* 13 (1997) 3944.
- [30] M.H. Schoenfish, J.E. Pemberton, *J. Am. Chem. Soc.* 120 (1998) 4502.
- [31] F. Porta, G. Speranza, Ž. Krpetić, V.D. Santo, P. Francescato, G. Scari, *Mater. Sci. Eng. B* 140 (2007) 187.
- [32] L. Burt, C. Gutierrez-Wing, M. Miki-Yoshida, M. Jose-Yacamán, *Langmuir* 26 (2004) 11778.
- [33] L. Fabris, S. Antonello, L. Armelao, R.L. Donkers, *J. Am. Chem. Soc.* 128 (2005) 326.
- [34] D.V. Leff, L. Brandt, J.R. Heat, *Langmuir* 12 (1996) 4723.
- [35] S.Y. Lin, Y.T. Tsai, C.C. Chen, C.M. Lin, C. Chen, *J. Phys. Chem. B* 108 (2004) 2134.
- [36] Z.P.P. Surujpaul, C. Gutiérrez-Wing, B. Ocampo-García, F. de M. Ramírez, C. Arteaga de Murphy, M. Pedraza-López, M.A. Camacho-López, G. Ferro-Flores, *Biophys. Chem.* 138 (2008) 83.
- [37] Ž. Krpetić, P. Nativo, F. Porta, M. Brust, *Bioconjugate Chem.* 20 (2009) 619.
- [38] D. Lin-Vien, N.B. Colthup, W.G. Fatley, J.G. Grasselli, *The Handbook of Infrared and Raman Characteristic Frequencies of Organic Molecules*, Academic Press, INC, Sand Diego/CA, 1991. p. 477.
- [39] S.L. Dawson, D.A. Tirrell, *J. Mol. Recogn.* 10 (1997) 18.
- [40] A. Ihs, B. Liedberg, *J. Colloid Interface Sci.* 44 (1991) 282.

Gold nanoparticles conjugated to Lanreotide peptide

E. M. Molina-Trinidad^{a,b}, O. Estévez-Hernández^{a,c}, L. Rendón^d, V. Garibay-Febles^e, E. Reguera^{a,c*}

^aCentro de Investigación en Ciencia Aplicada y Tecnología de Avanzada, IPN, Legaria 694, México, DF

^bFacultad de Estudios Superiores Cuautitlán, Universidad Nacional Autónoma de México, Estado de México, México

^cInstituto de Ciencia y Tecnología de Materiales (IMRE), Universidad de La Habana, Cuba

^dInstituto de Física, Universidad Nacional Autónoma de México, México D.F., México

^eInstituto Mexicano del Petróleo, Gustavo A. Madero, México D.F., México

Abstract

Lanreotide, a somatostatin analogue peptide used for peptide receptor mediated therapy in metastatic neuroendocrine tumors, was used as capping agent of gold nanoparticles (GNPs) obtained by citrate reduction method. The displacement of the citrate groups from the GNPs surface by lanreotide (LAN) molecules was evidenced by infrared and Raman spectra. The nanoparticles system, Au@LAN, was characterized from HRTEM (High-Resolution Transmission Electron Microscopy) and Z-contrast images, and UV-Vis, EDS spectra. The stability on aging in water solution of the composite is discussed from the UV-Vis spectra. The affinity constant of Au@LAN conjugate, calculated from Capillary Zone Electrophoresis data, was found to be 0,52. All the experimental evidence supports that the gold nanoparticles are effectively capped by the Lanreotide molecules through relatively strong covalent interactions. This result opens the possibility of combining the optical properties of gold nanoparticles and of Lanreotide molecule to form a bifunctional system for potential biomedical applications.

Keywords: Gold nanoparticles; Lanreotide peptide; Capping agents; Bioconjugate

*Corresponding Author: *E-mail address:* ereguera@yahoo.com (E. Reguera)

Anexo 3
Comprobación erogaciones del presupuesto otorgado para el Proyecto.
SEGUNDA ETAPA

a) Datos del Estudiante:

| a-1) Nombre | a-2) Especialidad | a-3) Apoyo otorgado \$ | | a-4) Descripción de su función dentro del proyecto. |
|---------------------|-------------------|------------------------|-----------|--|
| | | Importe mensual | Acumulado | |
| Adela Lemus Santana | Posdoctoral | 6,000 | 12,000 | Apoyo al proyecto en lo relativo en la preparación de muestras |
| 12,000 | | | | |

b) Servicios:

| b-1) Concepto | b-2) Cantidad | b-3) Importe | | b-4) Función o aplicación dentro del proyecto |
|--------------------------------|---------------|------------------|---------------|---|
| | | Importe Unitario | Importe Total | |
| Edilso Fco Reguera Ruiz | | | | |
| Estafeta Mexicana S.A. de C.V. | 1 | 185.99 | 185.99 | Envío de muestras para caracterización en el exterior |
| Estafeta Mexicana S.A. de C.V. | 1 | 184.88 | 184.88 | Envío de muestras para caracterización en el exterior |
| 370.87 | | | | |

d) Viajes realizados:

| d-1) Personal que viaja | d-2) Días | d-3) Importe | | d-4) Motivo del viaje y función para el desarrollo del proyecto. |
|--|------------------------|----------------|---------------|--|
| | | Importe por P. | Importe Total | |
| Jorge Roque de la Puente | 5 al 9 de julio | 5,330.01 | 5,330.01 | Asistir a la Habana, Cuba como ponente oral a la "Escuela y Taller sobre Nanotecnologías México-Cuba". |
| Adela Lemus Santana | 4 al 14 julio | 5,770.34 | 5,770.34 | Asistir como profesor a la Escuela Cubano-Mexicano de Nanociencia y Nanotecnología que sesionó a Universidad de la Habana donde impartió la conferencia. |
| Manuel Avila Santos | 20 al 28 de marzo | 10,434.30 | 10,434.30 | Visita al Laboratorio Nacional de Luz Síncrotron en Campinas, Brasil. |
| Sr. Andreas Stein Zhenzhen Stein (Pasajes) | 08 de febrero del 2011 | 8,693.71 | 8,693.71 | Conferencia a temas relacionados con el proyecto |
| Sr. Andreas Stein Zhenzhen Stein (Hospedaje) | 12 de enero del 2011 | 5,660.80 | 5,660.80 | Conferencia a temas relacionados con el proyecto |
| 35,889.16 | | | | |

e) Compras asociadas al proyecto

| e-1) Concepto | e-2) Cantidad | e-3) Importe | | e-4) Función o aplicación dentro del proyecto |
|-----------------------------|---------------|------------------|---------------|---|
| | | Importe Unitario | Importe Total | |
| Edilso Fco Reguera Ruiz | | | | |
| Infra, S.A. de S.V. | 1 | 9,237.04 | 9,237.04 | Material para síntesis y caracterización de muestras. |
| Infra, S.A. de S.V. | 1 | 25,519.95 | 25,519.95 | Material para síntesis y caracterización de muestras. |
| Sigma Aldrich, S.A. de C.V. | 1 | 4,027.52 | 4,027.52 | Material para síntesis y caracterización de muestras. |
| Sigma Aldrich, S.A. de C.V. | 1 | 846.80 | 846.80 | Material para síntesis y caracterización de muestras. |
| Office Depot | 1 | 426.00 | 426.00 | Material para síntesis y caracterización de muestras. |
| Alejandro Aguilar Nava | 1 | 1,999.99 | 1,999.99 | Material para síntesis y caracterización de muestras. |
| Edilso Fco Reguera Ruiz | | | | Material para síntesis y caracterización de muestras. |
| Infra, S.A. de S.V. | 1 | 9,237.08 | 9,237.08 | Material para síntesis y caracterización de muestras. |
| Infra, S.A. de S.V. | 1 | 4,746.64 | 4,746.64 | Material para síntesis y caracterización de muestras. |
| Cerrajería plata | 1 | 65.61 | 65.61 | Material para síntesis y caracterización de muestras. |
| Digital Print Defensa | 1 | 219.82 | 219.82 | Material para síntesis y caracterización de muestras. |
| El Crisol S.A. de C.V. | 1 | 2,998.72 | 2,998.72 | Material para síntesis y caracterización de muestras. |
| Sigma Aldrich, S.A. de C.V. | 1 | 1,873.40 | 1,873.40 | Material para síntesis y caracterización de muestras. |
| Sigma Aldrich, S.A. de C.V. | 1 | 2,607.68 | 2,607.68 | Material para síntesis y caracterización de muestras. |
| Sigma Aldrich, S.A. de C.V. | 1 | 1,933.72 | 1,933.72 | Material para síntesis y caracterización de muestras. |
| 65,739.97 | | | | |

Anexo 3
Comprobación erogaciones del presupuesto otorgado para el Proyecto.
CONCENTRADO FINANCIERO FINAL

a) Datos del Estudiante:

| a-1) Nombre | a-2) Especialidad | a-3) Apoyo otorgado \$ | | a-4) Descripción de su función dentro del proyecto. |
|---------------------|-------------------|------------------------|-----------|--|
| | | Importe mensual | Acumulado | |
| Adela Lemus Santana | Posdoctoral | 6,000 | 6,000 | Apoyo al proyecto en lo relativo en la preparación de muestras |
| Adela Lemus Santana | Posdoctoral | 6000 | 6,000 | Apoyo al proyecto en lo relativo en la preparación de muestras |

12,000

b) Servicios:

| b-1) Concepto | b-2) Cantidad | b-3) Importe | | b-4) Función o aplicación dentro del proyecto |
|--------------------------------|---------------|------------------|---------------|---|
| | | Importe Unitario | Importe Total | |
| Edilso Fco Reguera Ruiz | | | | |
| Estafeta Mexicana S.A. de C.V. | 1 | 185.99 | 185.99 | Envío de muestras para caracterización en el exterior |
| Estafeta Mexicana S.A. de C.V. | 1 | 184.88 | 184.88 | Envío de muestras para caracterización en el exterior |

370.87

d) Viajes realizados:

| d-1) Personal que viaja | d-2) Días | d-3) Importe | | d-4) Motivo del viaje y función para el desarrollo del proyecto. |
|--|------------------------|----------------|---------------|--|
| | | Importe por P. | Importe Total | |
| Blanca Zamora Reynoso | 1 año | 11,000.00 | 11,000.00 | Asistir a un adiestramiento en técnicas para estudios de superficie en la universidad de Southampton, Inglaterra. |
| Jorge Roque de la Puente | 5 al 9 de julio | 5,330.01 | 5,330.01 | Asistir a la Habana, Cuba como ponente oral a la "Escuela y Taller sobre Nanotecnologías México-Cuba". |
| Adela Lemus Santana | 4 al 14 julio | 5,770.34 | 5,770.34 | Asistir como profesor a la Escuela Cubano-Mexicano de Nanociencia y Nanotecnología que sesionó a Universidad de la Habana donde impartió la conferencia. |
| Manuel Avila Santos | 20 al 28 de marzo | 10,434.30 | 10,434.30 | Visita al Laboratorio Nacional de Luz Síncrotron en Campinas, Brasil. |
| Sr. Andreas Stein Zhenzhen Stein (Pasaaje) | 08 de febrero del 2011 | 8,693.71 | 8,693.71 | Conferencia a temas relacionados con el proyecto |
| Sr. Andreas Stein Zhenzhen Stein (Hospedaje) | 12 de enero del 2011 | 5,660.80 | 5,660.80 | Conferencia a temas relacionados con el proyecto |

46,889.16

e) Compras asociadas al proyecto

| e-1) Concepto | e-2) Cantidad | e-3) Importe | | e-4) Función o aplicación dentro del proyecto |
|-----------------------------|---------------|------------------|---------------|---|
| | | Importe Unitario | Importe Total | |
| Edilso Fco Reguera Ruiz | | | | |
| Infra, S.A. de S.V. | 1 | 9,237.04 | 9,237.04 | Materiales para síntesis y caracterización de muestras. |
| Infra, S.A. de S.V. | 1 | 25,519.95 | 25,519.95 | Materiales para síntesis y caracterización de muestras. |
| Sigma Aldrich, S.A. de C.V. | 1 | 4,027.52 | 4,027.52 | Materiales para síntesis y caracterización de muestras. |
| Sigma Aldrich, S.A. de C.V. | 1 | 846.80 | 846.80 | Materiales para síntesis y caracterización de muestras. |
| Office Depot | 1 | 426.00 | 426.00 | Materiales para síntesis y caracterización de muestras. |
| Alejandro Aguilar Nava | 1 | 1,999.99 | 1,999.99 | Materiales para síntesis y caracterización de muestras. |
| Edilso Fco Reguera Ruiz | | | | Materiales para síntesis y caracterización de muestras. |
| Infra, S.A. de S.V. | 1 | 9,237.08 | 9,237.08 | Materiales para síntesis y caracterización de muestras. |
| Infra, S.A. de S.V. | 1 | 4,746.64 | 4,746.64 | Materiales para síntesis y caracterización de muestras. |
| Cerrajería plata | 1 | 65.61 | 65.61 | Materiales para síntesis y caracterización de muestras. |
| Digital Print Defensa | 1 | 219.82 | 219.82 | Materiales para síntesis y caracterización de muestras. |
| El Crisol S.A. de C.V. | 1 | 2,998.72 | 2,998.72 | Materiales para síntesis y caracterización de muestras. |
| Sigma Aldrich, S.A. de C.V. | 1 | 1,873.40 | 1,873.40 | Materiales para síntesis y caracterización de muestras. |
| Sigma Aldrich, S.A. de C.V. | 1 | 2,607.68 | 2,607.68 | Materiales para síntesis y caracterización de muestras. |
| Sigma Aldrich, S.A. de C.V. | 1 | 1,933.72 | 1,933.72 | Materiales para síntesis y caracterización de muestras. |

65,739.97